Design of High-Energy Escape Trajectories with Lunar Gravity Assist

By Lorenzo CASALINO,[1)] and Lucio FILIZOLA[1)]

[1)]*Politecnico di Torino, Torino, Italy*

This paper presents a procedure for design and optimization of maneuvers for Earth escape with lunar gravity assist, to be used for interplanetary missions. In particular, focus is on missions to near-Earth asteroids with electric propulsion. The analysis treats the geocentric escape maneuver and the interplanetary flight separately, according to the patched-conic approximation. An indirect optimization method is used to maximize the final mass of the interplanetary leg for given escape C3 and mass. The analysis is conducted for different escape dates and provides final mass and components of the escape velocity. An approximate analysis method is developed to check the feasibility of a lunar gravity assist to improve the escape maneuver, for the considered escape date. If suitable opportunities are found, the indirect optimization method is again used to optimize the escape sequence, using the results of the approximate analysis to find a suitable tentative solution that permits convergence. Test cases are illustrated to highlight the benefit of lunar gravity assist maneuvers for the considered interplanetary transfer.

Key Words: Earth escape, Lunar gravity assist, Indirect optimization, Interplanetary missions

Nomenclature

A	:	azimuth
a	:	semimajor axis
$\boldsymbol{a}_p$	:	perturbations
c	:	effective exhaust velocity
$c_{a,b,c}$	:	equation coefficients
e	:	eccentricity
i	:	inclination
i_a	:	ascending node identifier
i_z	:	escape z-direction identifier
$k_{a,b,c}$	:	equation coefficients
m	:	mass
$\boldsymbol{r}$	:	position
$\boldsymbol{T}$	:	thrust
t	:	time
u	:	radial velocity component
$\boldsymbol{u}_h$	:	angular momentum unit vector
$\boldsymbol{u}_n$	:	ascending node unit vector
$\boldsymbol{V}$	:	velocity
v	:	eastward velocity component
w	:	northward velocity component
α	:	escape asymptote-ascending node angle
β	:	escape asymptote misalignment
γ	:	flight path angle
δ	:	velocity rotation
μ_M	:	Moon's gravitational parameter
ν	:	true anomaly
Φ	:	hyperbola half-angle
φ_L	:	launch site latitude
Ω	:	right ascension of ascending node
ω	:	argument of periapsis

Subscripts

$-$	:	before flyby
$+$	:	after flyby
0	:	start of heliocentric leg
1	:	perigee-Moon leg
2	:	Moon-escape leg
A	:	asteroid
c	:	circular
d	:	upper stage dry mass
E	:	Earth
esc	:	escape
f	:	end of heliocentric leg
M	:	Moon
p	:	perigee
PAF	:	payload attach fitting
ps	:	periselenium
u	:	useful mass on 200-km parking orbit
z	:	z-axis component
∞	:	Moon flyby relative velocity

1. Introduction

Lunar gravity assist (LGA) is a means to boost the energy and C3, that is, the square of the escape velocity, of an escape maneuver, thus improving the useful mass for a mission to a specific target. This strategy has been used in the past both for missions with low positive values of C3 (STEREO) and larger C3 values (ISEE-3, Nozomi).

Exploration of the solar system requires relatively large values of escape energy. The escape mass that a given launcher can provide with a direct launch is a decreasing function of the energy. However, the escape velocity can be properly directed to reduce the propellant consumption of the heliocentric flight, so an optimal trade-off usually exists. When the heliocentric flight employes a propulsion system with larger specific impulse compared to the launcher (e.g., electric propulsion), an interplanetary transfer to a near Earth target typically requires escape C3 of a few $(\mathrm{km/s})^2$. Lunar-gravity-assist (LGA) maneuvers can be used for a free increase of the escape C3, and the design of LGA escape trajectories for interplanetary missions is the object of the present paper. Most of the literature has concerned low energy trajectories, and only a limited number of papers can be found on high energy escape,[1–4)] which is instead of interest in the present analysis. The usual approach is to map

escape C3 as a function of date (i.e., position of the Moon along its orbit) and C3 value before the flyby, and eventually couple these results with the analysis of the interplanetary leg.

Preliminary design of interplanetary missions is usually carried out with the patched-conic approximation, and the geocentric escape maneuver is treated separately from the heliocentric leg. This approach is adopted also here. An indirect method[5,6] is used to optimize the geocentric and heliocentric phases. The design procedure proposed here starts from the optimization of heliocentric legs for different values of departure date and magnitude of hyperbolic excess velocity. It is not difficult to find a suitable tentative solution for the heliocentric leg, and convergence is extremely fast. Escape conditions are obtained for each trajectory, and feasibility of a gravity assisted escape maneuver is evaluated with an approximate analysis, which estimates the escape mass. Since the procedure is analytical, computational time for the approximate LGA analysis is negligible. The most interesting solutions can be optimized and verified by the indirect optimization method. A refinement of the results can finally be obtained by re-optimizing the heliocentric leg with the new escape conditions (i.e., mass and velocity at the end of the geocentric leg).

Analysis of the escape maneuver is treated with the same indirect optimization method used for the heliocentric legs, but finding a tentative solution that allows for convergence is a more difficult task, at least in the case of LGA escape. Additional complexity arises for missions to Near-Earth asteroids, as the hyperbolic excess velocity is typically used to rotate the orbit plane (with respect to the ecliptic) rather than change its energy, and has usually a large component perpendicular to the equator or Moon's orbital plane; the escape maneuver is therefore three-dimensional. The approximate analysis introduced here provides performance estimation for a preliminary evaluation of escape opportunities, but it also gives initial conditions that can be used to build a tentative solution for the indirect optimization of the geocentric leg, facilitating convergence.

2. Indirect Optimization of Heliocentric Trajectories

According to the patched-conic approximation, during the heliocentric flight the spacecraft is subject to the gravity of the sun alone. In the vicinity of a planet (i.e., inside its sphere of influence) only the planet's gravity is considered. The planets' spheres of influence are small compared to heliocentric distances and their dimension is neglected in preliminary design; asteroids do not have a sphere of influence as their gravity is negligible. Heliocentric legs connect at encounters with relevant bodies (planets, asteroids, etc.). The relative velocity at encounter is the hyperbolic excess velocity.

A point-mass spacecraft with variable mass is considered. Position $\boldsymbol{r}$, velocity $\boldsymbol{V}$ and mass m of the spacecraft are the problem state variables. Normalized values are employed, using the radius of Earth's orbit, the corresponding initial velocity and the spacecraft initial mass as reference values. The state differential equations are

$$\mathrm{d}\boldsymbol{r}/\mathrm{d}t = \boldsymbol{V} \tag{1}$$

$$\mathrm{d}\boldsymbol{V}/\mathrm{d}t = -\boldsymbol{r}/r^3 + \boldsymbol{T}/m \tag{2}$$

$$\mathrm{d}m/\mathrm{d}t = -T/c \tag{3}$$

The trajectory is controlled by the thrust vector $\boldsymbol{T}$ (the effective exhaust velocity c is constant). Boundary conditions require at escape $\boldsymbol{r}_0 = \boldsymbol{r}_E(t_0)$; the magnitude of the hyperbolic excess velocity and the initial mass are specified through $[\boldsymbol{V}_0 - \boldsymbol{V}_E(t_0)]^2 = V_{esc}^2$ and $m_0 = 1$. At rendezvous with the target asteroid, $\boldsymbol{r}_f = \boldsymbol{r}_A(t_f)$ and $\boldsymbol{V}_f = \boldsymbol{V}_A(t_f)$ are imposed. The final mass m_f is maximized with an indirect optimization method,[5,6] that provides the optimal escape date and the corresponding escape velocity components in the heliocentric frame; the optimal control history is also obtained. Additional constraints can be introduced to specify departure and/or arrival date, or time of flight. The hyperbolic excess velocity components can also be specified. A reference initial mass of 10000 kg is used for the preliminary calculations. The escape mass provided by the optimization of the escape maneuver, with the corresponding velocity components, is instead used in the refinement phase. A procedure based on Newton's method[7] is employed to solve the boundary value problem produced by the application of the theory of optimal control.

3. LGA Escape Trajectories

The purpose of this paper is the design of suitable LGA trajectories that attain given escape conditions. At the escape time, the spacecraft must reach the boundary of Earth's sphere of influence, here set at 1 million km, and the velocity (relative to the Earth) components in the J2000 heliocentric ecliptic frame are specified. For the analysis of the geocentric trajectory, variables are made non-dimensional by using the Earth equatorial radius and the corresponding circular velocity as reference values. Position and velocity of the Moon at escape time are obtained from JPL Ephemerides[8] DE405. The osculating orbit is used for Keplerian propagation of Moon's motion. The approximate analysis is carried out with a reference frame based on Moon's osculating orbit: x-axis towards the ascending node of Moon's orbit with respect to Earth's equator, z-axis along angular momentum, y-axis to complete a right-handed reference frame: $\boldsymbol{V}_{esc}$ is the escape velocity vector expressed in this frame.

The approximate analysis is based on a patched-conic approximation that neglects the dimension of Moon's sphere of influence. The trajectory is split into two geocentric legs. The inner leg goes from trajectory perigee (usually imposed by the launcher) to the Moon, the outer leg from the Moon to the boundary of Earth's sphere of influence (1 million km) where the escape velocity required by the heliocentric trajectory must be met at the specified escape time. LGA is modeled as a relative velocity rotation at Moon's intercept, which separates the geocentric legs. The leg from the Moon to escape (subscript 2) is first considered.

3.1. Moon to Escape

Moon's orbit is on the x-y reference plane and the intercept point must coincide with one of the nodes of the spacecraft escape hyperbola. The sign of the escape velocity component along the z-axis $v_{esc,z}$ determines where the ascending node must be positioned with respect to the direction of the outgoing asymptote: escape and ascending node must be on the same side for positive $v_{esc,z}$ (an index $i_z = +1$ is introduced to denote

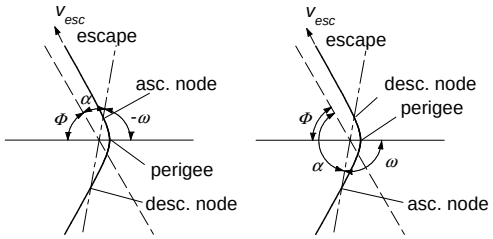

Fig. 1. Geometry of generic escape hyperbola for positive $v_{esc,z}$ (left) and negative $v_{esc,z}$ (right).

this situation) and on opposite sides in the other case ($i_z = -1$). The position of the ascending node, that is, the RAAN value Ω_2, defines the flyby point. The remaining orbital parameters of the hyperbola are consequently determined, once Ω_2 is selected.

Energy and semimajor axis depend on the escape velocity

$$a_2 = -\frac{1}{v_{esc}^2 - 2/r_{esc}} \tag{4}$$

A unit vector pointing to the ascending node $\boldsymbol{u}_n$ (components along x, y and z are $\cos\Omega_2$, $\sin\Omega_2$, and 0, respectively) defines the remaining orbital elements: first, the angle between ascending node and escape velocity $\alpha = \cos^{-1}(\boldsymbol{u}_n \cdot \boldsymbol{v}_{esc}/v_{esc})$ is determined. Then, the unit vector along angular momentum $\boldsymbol{u}_h$ is computed, as it is parallel to $i_z(\boldsymbol{u}_n \times \boldsymbol{v}_{esc})$. The inclination is thus related to the angular momentum component along the z-axis

$$i_2 = \cos^{-1}(u_{h,z}) \tag{5}$$

Since the flyby is at a node, one has (see Fig 1) either $\alpha + \Phi - \omega_2 = \pi$ (positive $v_{esc,z}$) or $\alpha - \Phi + \omega_2 = \pi$ (negative $v_{esc,z}$), where the hyperbola half-angle $\Phi = \cos^{-1}(1/e_2)$ has been introduced. The distance from the Earth must be the same for spacecraft and Moon at flyby, that is,

$$r_M = \frac{a_2(1-e_2^2)}{1 + e_2\cos\nu_2} \tag{6}$$

In general, flyby can occur at either node for any $v_{esc,z}$, with the true anomaly at flyby $\nu_2 = -\omega_2$ (flyby at ascending node, $i_a = +1$) or $\nu_2 = -\omega_2 + \pi$ (descending node, $i_a = -1$). However, flyby at descending node for positive $v_{esc,z}$ and at ascending node for negative $v_{esc,z}$ cannot take place if $\nu_2 < -\Phi$.

By manipulating these equations one gets

$$i_a i_z \sin\alpha \sqrt{e_2^2 - 1} = -(1 - i_a\cos\alpha) - (a_2/r_M)(e_2^2 - 1) \tag{7}$$

which is squared to obtain a quadratic equation in $e_2^2 - 1$

$$c_a(e_2^2-1)^2 + c_b(e_2^2-1) + c_c = 0 \tag{8}$$

with

$$c_a = (a_2/r_M)^2 \tag{9}$$

$$c_b = 2(a_2/r_M)(1 - i_a\cos\alpha) - \sin^2\alpha \tag{10}$$

$$c_c = (1 - i_a\cos\alpha)^2 \tag{11}$$

The quadratic equation is solved to obtain

$$e_2 = \sqrt{1 + \frac{-c_b \pm \sqrt{c_b^2 - 4c_a c_c}}{2c_a}} \tag{12}$$

The largest of the two solutions given by Eq. (12) (plus sign) is the only admissible solution of the radical equation (7) when the coefficient of $e_2^2 - 1$ and $\sqrt{e_2^2 - 1}$ in Eq. (7) have the same sign: since $a_2 < 0$, this occurs when $i_a i_z = +1$, that is, for flyby at ascending node and positive $v_{esc,z}$ or flyby at descending node and negative $v_{esc,z}$. The lower solution (minus sign) must instead be selected when flyby and escape are on opposite sides with respect to the direction of the outgoing asymptote. This solution, as already highlighted, does not exist when the hyperbola crosses the reference plane only once, that is, when $\nu_2 < -\Phi$. Once e_2 has been determined, Φ, ω_2, and ν_2 are immediately obtained.

Once the orbital elements are known, one can easily obtain the relative velocity at Moon's flyby $\boldsymbol{V}_{\infty+}$. This analysis can be performed for any flyby position (i.e. Ω_2); however, an iterative procedure is required to determine the feasible flyby when the escape time is specified, in dependence of the actual Moon's position at the relevant time. The analysis considers flyby at both ascending and descending node. Starting from a tentative value for Ω_2, ome computes the orbital parameters and the time of flight from the Moon to the boundary of the sphere of influence (1 million km, here), where escape is assumed to occur. The actual Moon's position at the flyby time is thus determined and defines the new value of Ω_2. A few iterations are typically required to obtain convergence. For the sake of simplicity, Moon's orbit is assumed to be circular to compute r_M and the relative velocity vector.

It is important to note that there is a misalignment between the velocity directions at infinity and at the boundary of the sphere of influence, that is, $\beta = (\pi/2 - \nu_{esc} + \gamma_{esc}) - \Phi$. At escape, the true anomaly is obtained from

$$r_{esc} = \frac{a_2(1-e_2^2)}{1 + e_2\cos\nu_{esc}} \tag{13}$$

and the flight path angle is

$$\gamma_{esc} = \tan^{-1}\frac{e_2\sin\nu_{esc}}{1 + e_2\cos\nu_{esc}} \tag{14}$$

Instead of numerically solving for the orbital elements that achieve the correct orientation of the escape velocity, β is added to the rotation that must be provided by Moon's flyby, as discussed later.

3.2. Perigee to Moon

The ΔV_p to transfer the spacecraft from a circular parking orbit to the trajectory towards the Moon defines the escape mass. The ΔV_p can be split into multiple burns as discussed later. The escape maneuver begins at the end of the last upper-stage burn and it is assumed that the spacecraft is at the perigee of its trajectory. The trajectories from perigee to the Moon (subscript 1) that allow feasible flybys to match the escape conditions are here found. Intercept is again on the reference plane and must therefore occur at a node of the spacecraft orbit: $\Omega_1 = \Omega_2$ when the flyby is either at the ascending or at the descending node of both orbits, whereas $\Omega_1 = \Omega_2 + \pi$ when it is at the ascending node of one orbit and descending node of the other one.

The magnitude of the relative velocity before and after the flyby must be the same $V_{\infty-} = V_{\infty+}$. Assuming Moon's orbit to be circular

$$V_{\infty-}^2 = u^2 + (v - V_M)^2 + w^2 = V_{\infty+}^2 \tag{15}$$

where $V_M = \sqrt{1/r_M}$ is Moon's circular velocity. The radial, eastward and northward components of the spacecraft velocity at Moon' encounter are

$$u = \sqrt{1/r_p/(1+e_1)}e \sin \nu_1 \tag{16}$$

$$v = \sqrt{1/r_p/(1+e_1)}(1+e_1 \cos \nu_1)\cos i_1 \tag{17}$$

$$w = i_a \sqrt{1/r_p/(1+e_1)}(1+e_1 \cos \nu_1)\sin i_1 \tag{18}$$

where ν_1 is the true anomaly at flyby of the perigee-Moon trajectory.

Substitution gives the radical equation

$$(V_{\infty+}^2 - 3/r_M) + (1-e_1)/r_p = \\ = -2\sqrt{r_p/r_M^3}\cos i_1 \sqrt{1+e_1} \tag{19}$$

which becomes the quadratic equation

$$k_a e_1^2 + k_b e_1 + k_c = 0 \tag{20}$$

with

$$k_a = (1/r_p)^2 \tag{21}$$

$$k_b = -4r_p \cos^2 i_1/r_M^3 - 2/r_p^2 - 2(v_{inf}^2 - 3/r_M)/r_p \tag{22}$$

$$k_c = (v_{inf}^2 - 3/r_M)^2 + 2(v_{inf}^2 - 3/r_M)/r_p + \\ 1/r_p^2 - 4r_p \cos^2 i_1/r_M^3 \tag{23}$$

Among the solutions

$$e_1 = \frac{-k_b \pm \sqrt{k_b^2 - 4k_a k_c}}{2k_a} \tag{24}$$

the larger one (plus sign) must be selected for $i_1 \le \pi/2$, whereas the correct solution is the lower one (minus sign) for retrograde orbits $i_1 \ge \pi/2$. From e_1, one has $a_1 = r_p/(1-e_1)$. The solution must be discarded for elliptical orbits ($a_1 > 0$) if the apogee $r_a = a_1(1+e_1)$ is lower than r_M. For acceptable solutions, $r_M = a_1(1-e_1^2)/(1+e_1\cos\nu_1)$ provides ν_1 (only outgoing trajectories are here considered and $0 < \nu_1 \le \pi$). The argument of periapsis is then determined, being $\nu_1 = -\omega_1$ (ascending node) or $\nu_1 = -\omega_1 + \pi$ (descending node).

Velocity rotation at flyby is given by the angle between the computed $\boldsymbol{V}_{\infty+}$ and $\boldsymbol{V}_{\infty-}$ vectors with the addition of the supplementary rotation β, as escape is actually reached at the boundary of the sphere of influence and not at infinity

$$\delta = \beta + \cos^{-1}[(\boldsymbol{V}_{\infty-} \cdot \boldsymbol{V}_{\infty+})/V_\infty^2] \tag{25}$$

According to the patched-conic approximation

$$\delta = 2\sin^{-1}\frac{\mu_M/r_{ps}}{V_\infty^2 + \mu_M/r_{ps}} \tag{26}$$

with μ_M being the Moon's gravitational parameter and r_{ps} the flyby periselenium, which can thus be determined. Trajectories are deemed feasible when the periselenium is at least 50 km above Moon's surface.

For any feasible flyby, the values of position and velocity at perigee (V_p) are evaluated and then rotated to the J2000 geocentric frame to determine the corresponding latitude, longitude and azimuth. The departure energy gives the required launch C3. Azimuth and $\Delta V_p = V_p - V_c$ can be used to evaluate the mass that the launcher can insert into the escape trajectory.

3.3. Verification

The most favorable escape trajectories are verified by numerical integration of the equations of motions in the EME2000 geocentric reference frame.

$$\mathrm{d}\boldsymbol{r}/\mathrm{d}t = \boldsymbol{v} \tag{27}$$

$$\mathrm{d}\boldsymbol{V}/\mathrm{d}t = -\boldsymbol{r}/r^3 + \boldsymbol{T}/m + \boldsymbol{a}_p \tag{28}$$

$$\mathrm{d}m/\mathrm{d}t = -T/c \tag{29}$$

Perturbations $\boldsymbol{a}_p$ from Moon's and sun's gravity, solar radiation pressure and nonsphericity of the Earth are considered. The Earth potential is described with the Earth Gravitational Model EGM2008, which provides normalized spherical harmonic coefficients for the Earth gravitational potential; terms up to the 8-th degree are considered.

The indirect method applied to the heliocentric leg could also be used for the optimization of the escape maneuver. However, in the present paper, a nonpropelled escape maneuver is considered and a simpler approach, which does not require optimization, can be used. In fact, if thrust is excluded and the departure inclination is specified, the number of boundary conditions (five conditions that fix initial inclination and escape radius and velocity components at the required escape time) exactly matches the number of free parameters (time, longitude, latitude, velocity magnitude and azimuth at departure) and a single solution exist. The same procedure based on Newton's method employed for the heliocentric leg is used to determine the initial unknowns, starting from the values provided by the approximate analysis.

4. Mission Design Procedure

Phasing loops are used to obtain the correct timing.[9] A direct launch to the Moon requires a strict timing and would have a very short launch window. It is instead assumed that the launcher parks the spacecraft into a 200-km circular orbit in the correct plane a few days before the actual start of the escape trajectory. The launcher upper stage performs a first impulsive maneuver at the proper location along the orbit, to place the spacecraft into an elliptic orbit with an apogee that is lower than the value corresponding to the trajectory to reach the Moon. Additional burns can be applied at each subsequent perigee passage to adjust the orbit period and obtain the correct timing, with the last one that achieves the required trajectory to the Moon at the proper time. This strategy allows for suitable launch windows, as the burn ΔVs can be adjusted to account for the actual launch conditions.

The useful mass that a launcher can deliver to a specific orbit depends on the energy of the trajectory and on the launch azimuth, but complete data for existing launcher and high-energy orbits are usually not available. They are instead often given for circular low Earth orbits (e.g., 200-km altitude). The following computations are here used to replicate the Delta IV Heavy performance.[11] The starting mass on the initial 200-km parking orbit is the sum of useful mass (m_u) and upper stage dry mass m_d (3550 kg). The useful mass given by NASA's Launch Vehi-

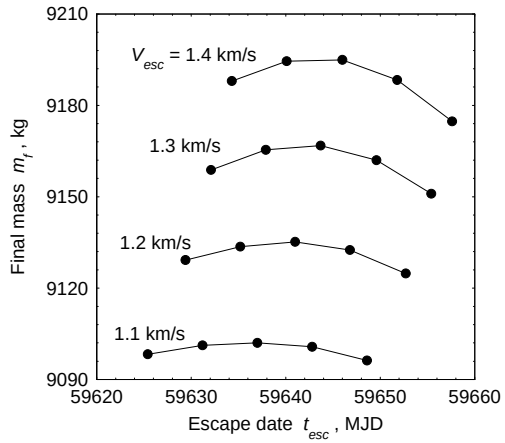

Fig. 2. Final mass of the heliocentric as a function of escape velocity and date for a 10000 kg initial mass.

cle Performance Website[10] is here approximated with the quadratic equation

$$m_u = 26280 - .6642(A - 90)^2 \tag{30}$$

where m_u is in kg and the azimuth A in degrees. The following burns sum up to $\Delta V = 1.05(V_p - V_c)$, that is the difference between the perigee velocity at the start of the trajectory to the Moon and the circular velocity on the parking orbit, with the addition of a 5 % margin. The useful escape mass is evaluated with the rocket equation

$$m_{esc} = (m_u + m_d)\exp[-\Delta V/c] - m_d - m_{PAF} \tag{31}$$

where the stage dry mass and the payload attach fitting mass (250 kg) are subtracted from the final mass. The stage effective exhaust velocity corresponds to a 460 s specific impulse.

The determination of suitable escape sequences starts from the analysis of the heliocentric leg. Trajectories with optimal departure date are found for different values of the escape velocity magnitude. The departure dates are then varied to evaluate the effect of performance (that is, the final mass). For each trajectory, the required escape conditions are also determined. Convergence is typically very fast and a few minutes are required for this analysis. The approximate analysis of the geocentric leg evaluates flyby feasibility (height on Moon's surface must be above 50 km), and provides the initial velocity V_p as a function of inclination i_1 with respect to the equatorial plane. Given the latitude of the launch site φ_L, launch azimuth is evaluated from

$$\cos i_1 = cos\varphi_L \sin A \tag{32}$$

to obtain an estimation of the escape mass. The best opportunities are then numerically verified with the perturbed dynamical model to obtain exact departure conditions and escape mass. The heliocentric legs for these escape conditions are finally reoptimized to obtain the actual mass delivered to the target asteroid.

5. Results

A mission to asteroid 2001 QJ_{142} with departure in early 2022 is presented as a test case. This asteroid is a possible alternative target for the Asteroid Robotic Redirect Mission (ARRM).

Table 1. Escape trajectories for V_{esc} = 1.2 km/s.

Items	Estimate	Actual
Launch C3, km^2/s^2	-1.27	-1.34
Launch longitude, deg	154	150
Launch latitude, deg	16	18
Periselenium, km	1989	1904
Escape mass, kg	10469	10480

Table 2. Escape trajectories for V_{esc} = 1.3 km/s.

Items	Estimate	Actual
Launch C3, km^2/s^2	-1.05	-1.13
Launch longitude, deg	162	159
Launch latitude, deg	13	15
Periselenium, km	1961	1898
Escape mass, kg	10435	10448

Table 3. Escape trajectories for V_{esc} = 1.4 km/s.

Items	Estimate	Actual
Launch C3, km^2/s^2	-0.76	-0.84
Launch longitude, deg	169	168
Launch latitude, deg	9	11
Periselenium, km	1965	1921
Escape mass, kg	10392	10403

Table 4. Summary of performance.

Items	Sol. 1	Sol. 2	Sol. 3
V_{esc} km/s	1.2	1.3	1.4
Escape start	2/26/22	2/26/22	2/27/22
Escape	3/8/22	3/8/22	3/8/22
Escape mass, kg	10480	10448	10403
Rendezvous	6/17/23	6/13/23	6/10/23
Final mass, kg	9561	9566	9556

Escape occurs in March 2022 with rendezvous with the target asteroid in June 2023. Performance of the heliocentric leg for a reference escape mass of 10000 kg are presented in Fig. 2. The heliocentric trajectory benefits from a higher escape energy, and the final mass grows with the escape velocity magnitude V_{esc}. However, lower escape masses are to be expected when V_{esc} grows and the actual escape mass must be used for a meaningful comparison.

Direct escape suffers from high energy and declination of the escape hyperbola well above 40 degrees, which forces a launch azimuth different from 90 degrees. Expected escape masses are below 9500 kg. When LGA is considered, solutions which combine eastward launch from Cape Kennedy (φ_L = 28.5 degrees) and low energy escape with C3 well below $-0.5\,km^2/s^2$ are found.

Estimations of the approximate analysis and results from the verification are compared in Tables 1-3 for the three best opportunities, corresponding to V_{esc} = 1.2, 1.3, 1.4 km/s, respectively. These trajectories require departure around MJD 59646 (March 8,2022) slightly later than the optimal date determined by the heliocentric leg optimization for the lower values of escape velocity. They have inclination equal to the latitude of the launch site for eastward launch and flyby at the ascending node (with respect to the plane of Moon's orbit) of both perigee-Moon and Moon-escape legs.

The estimations are sufficiently accurate to find suitable tentative solutions to assure convergence, even though the integra-

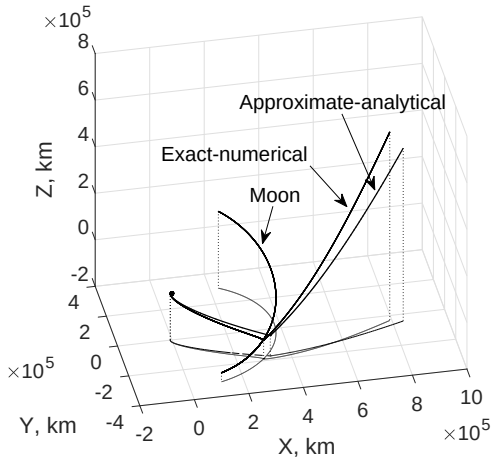

Fig. 3. Escape trajectories for V_{esc} = 1.3 km/s.

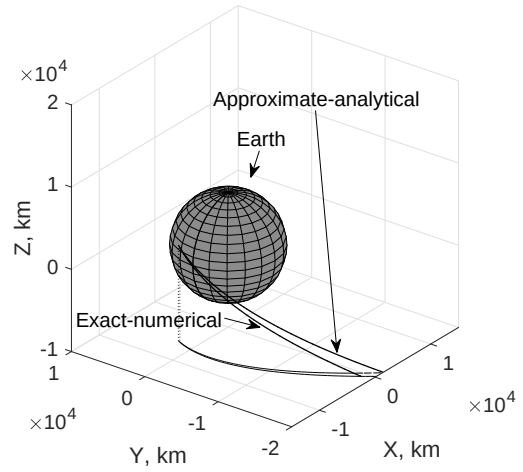

Fig. 4. Departure of escape trajectories for V_{esc} = 1.3 km/s.

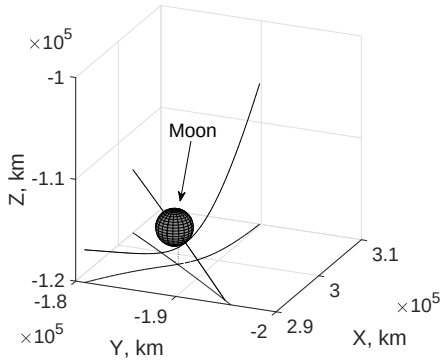

Fig. 5. Moon flyby of exact-numerical escape trajectory for V_{esc} = 1.3 km/s.

tion is numerically sensitive. Differences between the approximate and exact trajectories are essentially due to the assumption of circular Moon's orbit for the approximate analysis and, to a lesser extent, to the angle β and perturbations that affect the exact trajectory. Results of the re-optimization of the heliocentric leg for the selected escape maneuvers are presented in Table 4. The proposed procedure allows to find the optimal value of escape velocity for the proposed mission with a limited computational effort.

The globally optimal solution corresponds to $v_{esc,z}$ = 1.3 km/s and is presented in Figs. 3-5. The approximate and exact trajectories aim at slightly different points but the similarities of the solutions are evident. The trajectories after the flyby differ because of the angle β discussed before. Difference at departure are due to the different Moon distance in the two models, and in part to the effect of Earth oblateness. The exact solution can be used to identify the flyby geometry: the spacecraft passes below the Moon, to obtain the required high escape declination towards the northern hemisphere.

6. Conclusion

A procedure for the design of LGA escape maneuvers for interplanetary transfers has been presented. In contrast to existing methods, the proposed procedure starts from the analysis of the heliocentric leg with an indirect optimization method and then finds suitable escape maneuvers by means of an approximate analysis followed by numerical verification. The efficient indirect optimization of the heliocentric legs and the analytical approximate analysis of LGA escape maneuvers limit the computational effort. Results prove the effectiveness of the method, which can provide the globally optimal solution to target specific destinations in short times.

References

1) Campagnola, S., Jehn, R., and Corral Van Damme, C.: Batchelor, G. K.: Design of Lunar Gravity Assit for the BEPICOLOMBO Mission to Mercury, AAS Paper 04-130, 2004.
2) Landau, D., McElrath, T.P., Grebow, D., and Strange, N.J.: Efficient Lunar Gravity Assits for Solar Electric Propulsion Missions, Paper AAS 12-165, 2012.
3) McElrath, T.P., Lantoine, G., Landau, D. Grebow, D., Strange, N., Wilson, R., Sims, J., Using Gravity Assists in the Earth-Moon System as a Gateway to the Solar System, GLEX-2012.05.5.2x12358, 2012.
4) Lantoine, G., and . McElrath, T.P.: Families of Solar-Perturbed Moon-to-Moon Tranfers, Paper AAS 14-471, 2014.
5) Bryson, A.E., and Ho, Y.-C.: *Applied Optimal Control*, Cambridge University Press, London, 1967, pp.1–10.
6) Casalino, L., Colasurdo, G., and Pastrone, D.:"Optimal Low-Thrust Escape Trajectories Using Gravity Assist", *Journal of Guidance, Control, and Dynamics*, **22** (1999), pp. 637–642.
7) Colasurdo, G., and Pastrone, D.: Indirect Optimization Method for Impulsive Transfer, Paper AIAA 94-3762, 1994.
8) JPL Planetary and Lunar Ephemerides, https://ssd.jpl.nasa.gov/? planet_eph_export, accessed April 3, 2017.
9) Farquhar, R. W., and Dunham, D. W.: The Indirect Launch Mode: A New Launch Technique for Interplanetary Missions, *Acta Astronautica*, **45** (1999), pp. 491–497.
10) Launch Vehicle Performance Website, https://elvperf.ksc.nasa.gov/pages/Query.aspx, accessed April 3, 2017.
11) Delta IV launch Services User's Guide, United Launch Alliance, Centennial, CO, 2013.